ELSEVIER

Polymer 42 (2001) 289–295

polymer

www.elsevier.nl/locate/polymer

The pressure and temperature dependence of the relaxation processes in poly(methylmethacrylate)

S. Theobald*, W. Pechhold, B. Stoll

Department of Applied Physics, University of Ulm, D-89069 Ulm, Germany

Received 20 August 1998; received in revised form 22 March 2000; accepted 12 April 2000

Abstract

The motion of molecular segments in poly(methylmethacrylate) (PMMA) is investigated in dependence on temperature and hydrostatic pressure with dielectric and dynamic-mechanical experiments. Molecular motion can indirectly be seen in the specific volume and in the specific heat capacity. Relaxation times, usually plotted in activation diagrams, can be calculated by a detailed model for the molecular structure of the polymer melt, where the free-volume theory is replaced by the dislocation concept. The model allows us to correlate the thermal properties with the dynamic behavior, and is able to calculate specific heat capacity curves. © 2000 Published by Elsevier Science Ltd.

Keywords: Poly(methylmethacrylate); Pressure dependence of relaxation processes; Dislocation concept

1. Introduction

The freezing-in process in an amorphous polymer—this means the change from the molten to the glassy state—is characterized by some prominent experimental features:

- viscosity increases above a critical value;
- relaxation time of the system increases above a critical value;
- change in thermal expansion, compressibility and heat capacity.

The aim is to understand the nature of the transition and thus to correlate dynamic and thermal properties. Beyond the widely known theory of free volume [1], we use the dislocation concept based on the meander model [2], where the holes are represented by dislocations in the molecule bundles. Dislocations are known as lattice defects, which are important for the plastic deformation of metals. At first glance, it seems strange to use a similar concept in amorphous materials. Yet, some physicists are considering the liquid state as a crystal with an extremely high density of lattice defects, particularly dislocations [3,4]. Similarly, in the meander model, the amorphous state is described by introducing disorder in the regular packing of a bundle of molecules. It seems reasonable to use "dislocations" rather than "holes", to explain e.g. the shear deformation of the meander blocks (viscoelastic behavior) and the kinetics of the glass relaxation and its pressure dependence. The molecular mobility is described by only one variable, the density of these dislocations z. This theory was applied before successfully to other typical amorphous polymers (e.g. PVAc [5] and PS [6]) and was able to explain several factors affecting the glass relaxation (molecular weight, swelling, cross-linking, deformation amplitude and hydrostatic pressure). The emphasis of this work lies on the description of the freezing-in process in poly(methylmethacrylate) (PMMA) in dependence of hydrostatic pressure, taking the role of the local relaxation into account.

2. Experimental

2.1. Sample

PMMA was obtained from Röhm, Darmstadt in granular form. It has a molecular weight of $M_w = 150$ kg/mol and a dispersivity of $M_w/M_n \approx 2$.

2.2. Dilatometric experiments

Volume measurements were carried out in a pressure range from 0.1 to 700 MPa and in a temperature range from 0 to 220°C. In order to cover the whole pressure

* Corresponding author. Tel.: +49-731-5022950; fax: +49-731-5022958.

E-mail address: stefan.theobald@physik.uni-ulm.de (S. Theobald).

0032-3861/01/$ - see front matter © 2000 Published by Elsevier Science Ltd.
PII: S0032-3861(00)00317-7

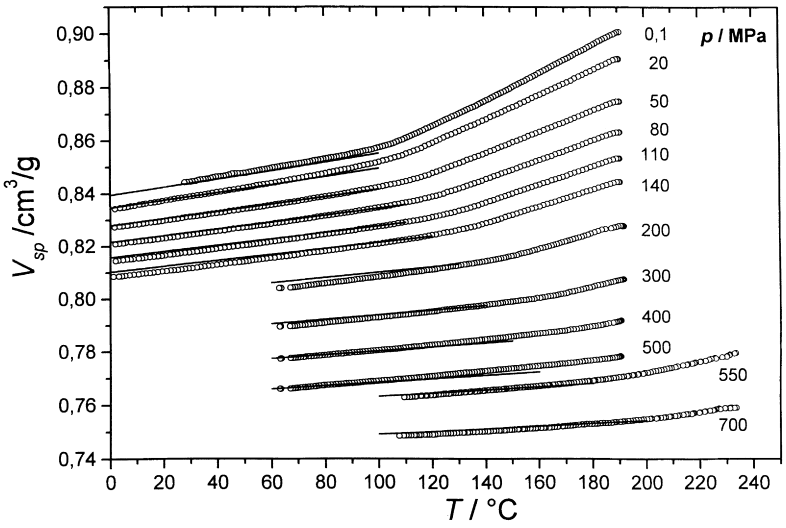

Fig. 1. Isobaric measurements of the specific volume of PMMA for the pressures indicated at the curves. The fully drawn lines are the fit of Eq. (4) to the experimental data. The parameters are given in Table 1.

range, we have used three experimental setups: a modified commercial Netzsch Dilatometer at ambient pressure, and two high-pressure dilatometers, which are piston cylinder devices with 6 mm (up to 200 MPa) and 22 mm (up to 1 GPa) diameter. They are described in detail elsewhere [7]. For isobaric measurements, pressure was adjusted in the molten state at high temperatures. Subsequently, the sample was cooled with a constant rate of 0.5 K/min. The results are shown in Fig. 1. The glass transition is characterized by the change in the slope (thermal expansion) of the curve. With increasing pressure, the glass transition shifts to higher temperatures and the change in the expansion coefficient decreases.

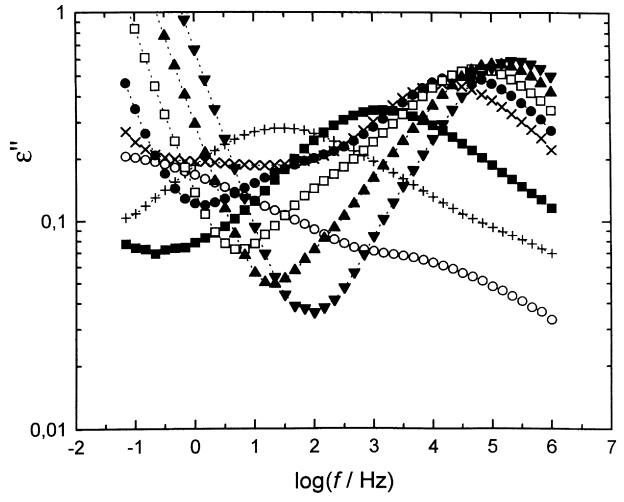

Fig. 2. The dielectric loss ϵ'' as a function of frequency at atmospheric pressure for the following temperatures—W: −24.0°C; +: 36.5°C; B: 83.2°C; ×: 119.3°C; X: 127.4°C; A: 135.5°C; O: 144.0°C; and P: 152.8°C.

2.3. Dielectric measurements

For preparing a sample capacitor, we pressed sheets of PMMA between plates of gold-plated steel (15 mm in diameter), using polyimid stripes (75 μm thick) as spacers, in a heating press for 1 h at 165°C. The dielectric measurement equipment (low-frequency bridge and Network analyzer system) and the pressure-generating system are reported in detail in another paper [8]. The sample capacitor was embedded in silicon oil as a pressure-transmitting medium. Conductivity measurements of silicon oil are also described in Ref. [8], where one can estimate the negligible influence of the pressure-transmitting medium on the results of the measurement.

Dielectric spectra were recorded at various temperatures (from −20 to 200°C) and hydrostatic pressures (up to 500 MPa) in a frequency range from 5×10^{-2} to 1×10^{6} Hz. Measurements of the dielectric loss at ambient pressure and different temperatures are shown in Fig. 2. Each spectrum is analyzed by the division into four contributions (as can be seen in Fig. 3): (a) the conductivity caused by free charges from impurities; (b) the cooperative reorientation of dipoles in the glass relaxation process; and (c), (d) local relaxation processes. For our analysis we use the additive superposition of Cole–Cole relaxation processes and therefore we get from the fit to the experimental data for each process the maximum frequency, the relaxation strength and the width.

2.4. Quartz-resonator method

The pressure dependence of the complex shear modulus can be measured using the quartz-resonator method, which is described in Ref. [9]. Plates (5 mm thick) of PMMA are coupled to both electrodes of a 3 MHz AT shear resonator. The same pressure vessel as for the dielectric experiment

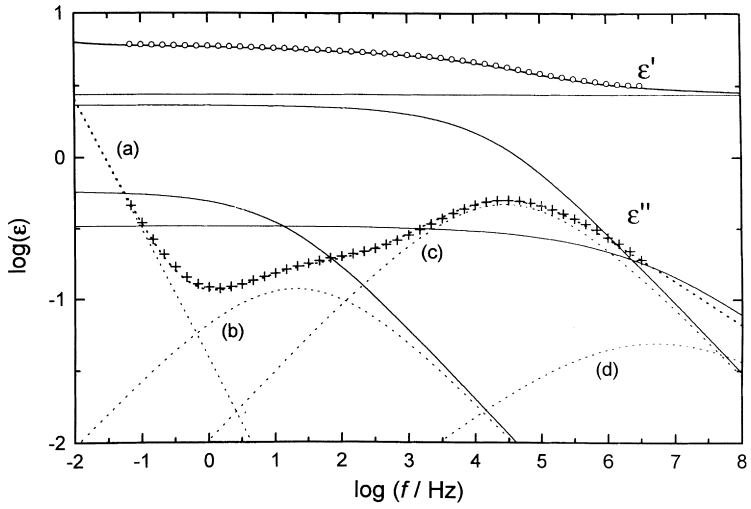

Fig. 3. Representation of the dielectric spectrum at $T = 151°C$ and a pressure of $p = 100$ MPa as a sum of four contributions (a) free charge carriers from impurities in the sample; (b) cooperative reorientation of segments in the glass relaxation process; (c) and (d) local relaxation processes.

can be used. Measurements of the shear modulus at two different temperatures are shown in Fig. 4. One notices the weak increasing of the real part of the shear modulus at high pressures.

3. Results and discussion

In this section we want to discuss our experimental results within the frame of a superstructural model of the polymer melt, the meander model.

3.1. The dislocation concept

Molecular motions, comparable with the dislocation movement in crystals, were considered in the dislocation concept in order to describe shear fluctuations. In the meander model, we assume that the polymer chains are arranged in parallel in the form of bundles and they are packed nearly hexagonally in spite of local defects, which are due to conformational changes in the amorphous state (Fig. 5, upper part). In the lower part of Fig. 5, two edge dislocations in a cross-section of two bundles are shown. It is likely that the dislocations associate in dislocation walls, where the regular packing of the chains is disturbed.

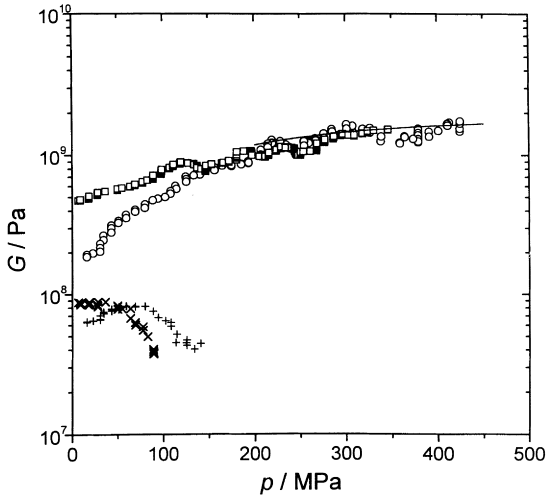

Fig. 4. The shear modulus, measured at a frequency of 3 MHz by a quartz-resonator method for PMMA as a function of pressure for two temperatures (A, ×: 159°C, W, +: 184°C). Upper curves: real part, and lower curves: imaginary part.

The concentration z of segments[1] within a dislocation wall is given by a Boltzmann factor.[2]

$$z = \exp\left(\frac{-\epsilon_s}{RT}\right) \tag{1}$$

The energy ϵ_s of a dislocation wall per segment area depends on the shear modulus G of the glassy state, the Burgers vector b (which is in the order of the chain distance d) and the Poisson ratio ν.

$$\epsilon_s = \frac{0.3Gb^2d}{4\pi(1-\nu)} \tag{2}$$

The pressure dependence of ϵ_s is described using a Grüneisen parameter [5]:

$$\frac{\epsilon_s(T,p)}{\epsilon_{s0}} = \left(\frac{V(T,p)}{V_0}\right)^{1-2\gamma_{disl}} \tag{3}$$

where, according to Pechhold [7]:

$$\frac{V(T,p)}{V_0} = \left\{1 + \frac{2\gamma}{K_0}[(p-p_0) - K_0\alpha_0(T-T_0)]\right\}^{-1/2\gamma} \tag{4}$$

Two different Grüneisen parameters have been used here:

[1] A chain segment consists of one or two monomeric units and should enable all possible types of conformations.

[2] The usually written denominator is just compensated by dislocation fluctuation in the wall.

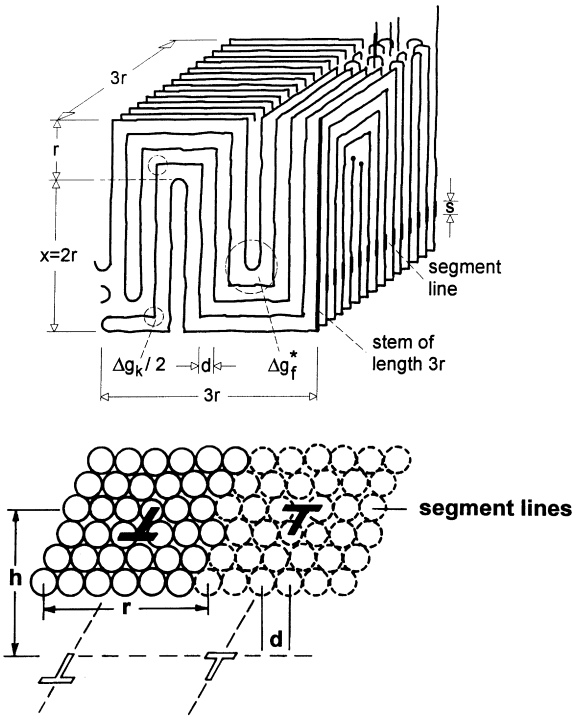

Fig. 5. Meander cube to define geometry and free energy contributions Δg_f^*, Δg_k of superfolding. Two different bundle segment lines and one cube segment line are shown. The cross-section of two bundles with a step dislocation in each are indicated.

γ for the bulk modulus, and γ_{disl} for the special elastic deformations near the dislocation core. The index zero refers to the reference temperature T_0 and pressure p_0. K is the bulk modulus, and α, the thermal expansion coefficient of the glassy state. Eq. (4) has been fitted to high pressure–volume data (Fig. 1) with the parameters in Table 1.

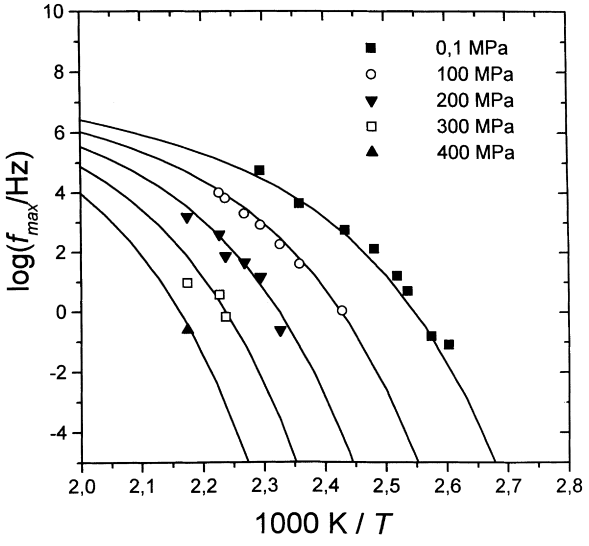

Fig. 6. Activation diagram (frequency of dielectric loss maximum versus reciprocal temperature) for the glass relaxation process for pressures of 0.1, 100, 200, 300 and 400 MPa.

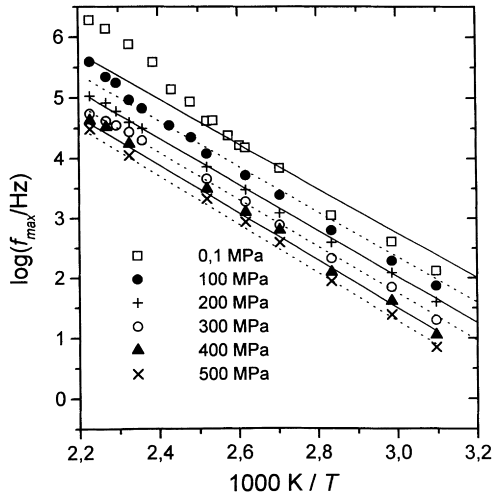

Fig. 7. Activation diagram for the local relaxation process for pressures of 0.1, 100, 200, 300, 400 and 500 MPa from dielectric measurements.

Due to the fact that the concentration of dislocations—which is in the melt in thermal equilibrium—is rather high ($z \approx 0.2$), the disordered packing of the chains in the amorphous bundle can be described by a network of dislocation walls. These play the role of the free volume.

In the meander model, the cooperative nature of the molecular motion is considered with the meander cube (size approximately 10–20 nm, Fig. 5) as the cooperative unit. One can propose that micro-Brownian motions are only possible if each segment line contains at least one segment in a dislocation wall [2]. This probability (for the whole cube) is given by the curved bracket in Eq. (5). The kinetics are given by an Arrhenius-type factor (intramolecular segmental jump) in Eq. (5). The following formula describes the frequency of maximum (dielectric) loss [2]:

$$f_m = \frac{f_0}{\pi} e^{-Q/RT} \{1 - (1 - z)^{3r/d}\}^{3(3r/d)^2 d/s} \quad (5)$$

Here f_0 = local vibration frequency; Q = local activation energy; d = mean distance between neighboring chains; s = length of a segment along the chain; and r = mean diameter of a bundle of macromolecules.

Eq. (5) has been fitted to the results of dielectric measurements on PMMA in Fig. 6 and the parameters are listed in Table 1. PMMA is one of the few examples where the dielectric local relaxation process is stronger than the glass relaxation process which was attributed to the special chemical structure of the side group in this polymer by many authors (see, for instance, Ref. [10]). The glass relaxation was separated from the local relaxation by fitting a sum of Cole–Cole processes to the experimental data, using a computer (Fig. 3). The activation diagram for the local relaxation (Fig. 7) was fitted by:

$$f_m = \frac{f_0}{\pi} e^{-Q/RT} \quad (6)$$

with the same parameters as in Eq. (5) (see Table 1).

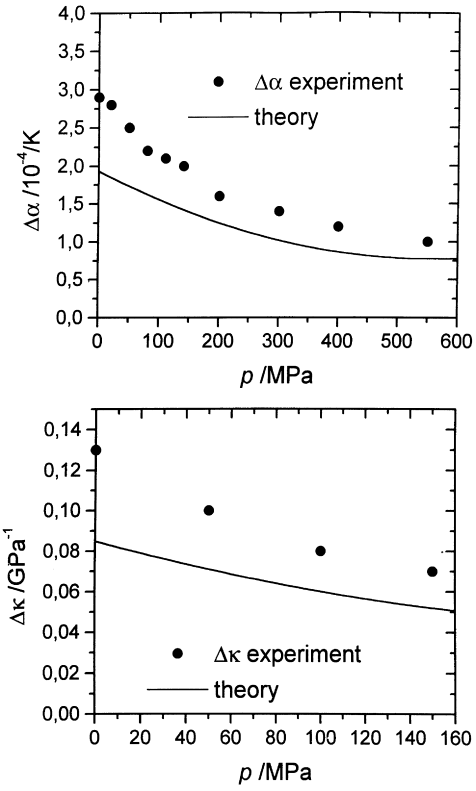

Fig. 8. The volume expansion coefficient and the isothermal compressibility of PMMA. The plots indicate the difference between the molten and the glassy state, $\Delta\alpha$, $\Delta\kappa$, taken at the dilatometric glass temperature as a function of pressure. Symbols: experimental data from Fig. 1, theoretical curves calculated according to Eqs. (10) and (11).

Deviations at high temperatures and low pressures in the thermal glass transition regime are an indication of the coupling between the molecular mechanisms of local and glass relaxation [10]. The local activation energy was assumed to include an intramolecular (pressure-independent) part and, therefore,

$$\frac{Q(T,p)}{Q_0} = 1 - \zeta + \zeta\frac{\epsilon_s(T,p)}{\epsilon_{s0}} \tag{7}$$

was assumed with $\zeta = 0.6$ as determined by measurements on swollen polymers [11]. All parameters are listed in Table 1. These parameters are consistent with other evaluations of the parameters of the molecular model [2,5,6,11]. A check of these parameters is possible for ϵ_s by Eq. (2) and for γ_{disl} using the high-frequency shear modulus measurements in Fig. 4. These tests showed good agreement. The size of the superstructural unit ($3r$) is also consistent with AFM images of the PMMA surface [12] and with the plateau compliance of the melt, if one assumes that in PMMA a shear motion is performed between bundles as a whole; this may be the consequence of a twisting of the macromolecules.

3.2. Calculation of thermodynamic properties

Using the same parameters as determined above, it is possible to calculate the contribution of the dislocations to the volume expansion coefficient, the compressibility and the specific heat capacity by the following equations, using an approximation for the Gibbs free energy [5] per segment:

$$g_s^* = 8z\epsilon_s + 8RT(z\ln z - z) \tag{8}$$

$$V_{\text{disl}} = \frac{\partial g^*}{\partial p} \tag{9}$$

$$\Delta\alpha = \frac{1}{V_s}\frac{\partial^2 g_s^*}{\partial p\,\partial T} \tag{10}$$

$$\Delta\kappa = -\frac{1}{V_s}\frac{\partial^2 g_s^*}{\partial p^2} \tag{11}$$

$$\Delta c_p = -\frac{T}{m_s}\frac{\partial^2 g_s^*}{\partial T^2} \tag{12}$$

where m_s is the mass of a segment. The comparison of the calculations to the experimental results (from Fig. 1) show (Fig. 8), that the dislocations form the major contribution to the change of thermodynamic properties at the glass transition.

3.3. Calculation of calorimetric cooling and heating curves

Moreover, it is possible to calculate the concentration of dislocations as a function of temperature and pressure during cooling and heating runs. This is done using a relaxation equation:

$$\frac{\mathrm{d}z}{\mathrm{d}t} = -\frac{1}{\tau_z}(z - z_{\text{eq}}) \tag{13}$$

for deviations from the thermal equilibrium, when $z = z_{\text{eq}}$. The "structural" relaxation time τ_z should be proportional to the dielectric relaxation time $\tau_{\text{diel}} = 1/(2\pi f_{max})$ by a constant factor, since a constant factor was also found between the dynamic-mechanical and the dielectric relaxation time in the glass process [5,6,11]. Therefore,

$$\tau_z = \frac{A}{2\pi f_{\max}} \tag{14}$$

Eqs. (13), (14) and (5) have been solved numerically to obtain the curves in Fig. 9. These curves show the typical behavior of volume–temperature diagrams near the glass transition, since:

$$V_{\text{disl}} = \frac{\partial g^*}{\partial p} = 8z\frac{\partial \epsilon_s}{\partial p} \tag{15}$$

where $\partial\epsilon_s/\partial p$ is almost constant. Similarly, we obtain the enthalpy contribution of the dislocations:

$$h_{\text{disl}} = g_s^* - T\frac{\partial g_s^*}{\partial T} = 8z\left(\epsilon_s - T\frac{\partial \epsilon_s}{\partial T}\right) \tag{16}$$

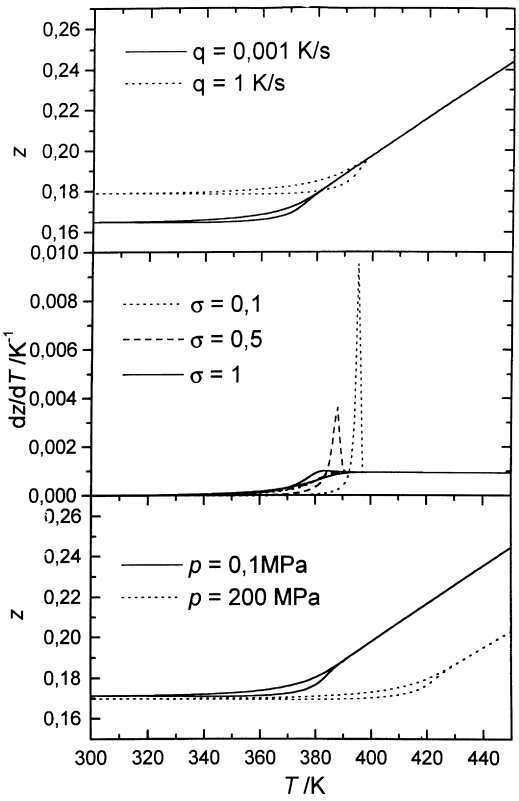

Fig. 9. The concentration z of dislocations per segment and its temperature derivative, $\partial z/\partial T$, as a function of temperature, calculated according to Eqs. (1), (5), (13) and (14). q = cooling rate, σ = parameter for the width of segment line fluctuations (see text).

Therefore, the specific heat capacity is given by:

$$c_p^{\mathrm{disl}} = \frac{1}{m_s}\frac{\partial h_{\mathrm{disl}}}{\partial T} = \frac{8}{m_s}\frac{\partial z}{\partial T}\left(\epsilon_s - T\frac{\partial \epsilon_s}{\partial T}\right) - \frac{8zT}{m_s}\frac{\partial^2 \epsilon_s}{\partial T^2} \quad (17)$$

Table 1
Parameters from the fit of theoretical curves to experimental data in Figs. 1, 6, 7 and 10

Parameter	Unit	Data
T_0	K	293
p_0	MPa	0.1
V_0	cm^3/g	0.8425
K_0	MPa	3189
$K_0\alpha_0$	MPa/K	0.593
γ		4.98
ζ		0.6
Q_0	kJ/mol	66.7
ϵ_{s0}	kJ/mol	5.62
f_0	Hz	3×10^{13}
$3r/d$		30
d	nm	0.88
s	nm	0.44
γ_{disl}		1.53
ν		0.33
A		10

where c_p^{disl} is approximately proportional to $\partial z/\partial T$. In Fig. 9, calculated curves for $\partial z/\partial T$ for different values of the parameter σ are shown. This parameter was introduced to account for the relaxation time distribution. This distribution is obtained in the meander model by fluctuations in the shape of the superstructural units, leading to a fluctuation of the length of segment lines, which is represented by a $3r/d$ distribution with a standard deviation of σ. For the theoretical curve in Fig. 10, the parameters listed in Table 1 have been chosen. The base line (c_p of the glass) has been fitted with additional parameters and (for better comparison) Δcp, which was calculated by Eq. (12), has been multiplied by 1.2. The parameter $A = 10$ is consistent with a comparison between dielectric and temperature-modulated DSC measurements [13,14]. Therefore, it is shown that the

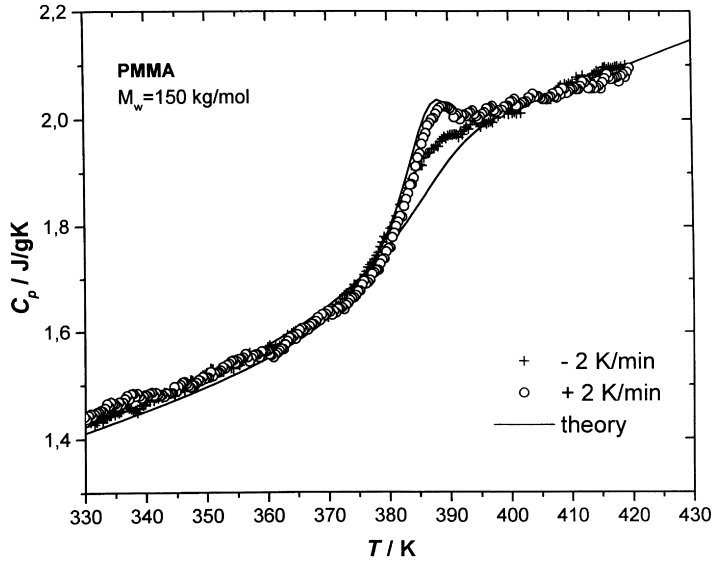

Fig. 10. The specific heat capacity of PMMA at atmospheric pressure. Symbols: measured by J.E.K. Schawe, University of Ulm at 2 K/min for heating and cooling. Drawn lines are calculated according to Eqs. (5), (13), (14) and (17).

dislocation concept predicts the main features of the thermal properties near T_g with the same parameters as for the activation diagram.

Acknowledgements

The authors are indebted to P.U. Mayr and A. Saier for the high pressure–volume data and to H.U. Scholl for the dielectric measurements. Financial support from the Deutsche Forschungsgemeinschaft (SFB 239) is gratefully acknowledged.

References

[1] Ferry JD. Viscoelastic properties of polymers. New York: Wiley, 1961.
[2] Pechhold W, Sautter E, Soden Wv, Stoll B, Grossmann HP. Makromol Chem Suppl 1979;3:247.
[3] Siol M. Z Phys 1961;164:93.
[4] Pechhold W, Grossmann HP, von Soden W. Colloid Polym Sci 1982;260:248.
[5] Heinrich W, Stoll B. Progr Colloid Polym Sci 1988;78:37.
[6] Barry S. Thesis, University of Ulm, 1992.
[7] Dollhopf W, Barry S, Strauß MJ. In: Hochheimer HD, Etters RD, editors. Frontiers of high pressure research, New York: Plenum Press, 1991.
[8] Heinrich W, Stoll B. Colloid Polym Sci 1985;263:873.
[9] Theobald S, Schwarzenberger P, Pechhold W. High Pressure Res 1994;13:133.
[10] Schmidt-Rohr K, Kulik AS, Beckham HW, Ohlemacher A, Pawelzik U, Boeffel C, Spiess HW. Macromolecules 1994;27:4733.
[11] Pechhold W, Böhm M, Soden Wv. Progr Colloid Polym Sci 1987;75:23.
[12] Zink B. University of Ulm, personal communication, 1997.
[13] Schawe JEK, Theobald S. J Non-Cryst Solids 1998;235–237:496.
[14] Hensel A, Schlick C. J Non-Cryst Solids 1998;235–237:510.